



Peer review status:

This is a peer-reviewed postprint submitted to EarthArXiv.

# 1 Winter subglacial meltwater detected in Greenland Fjord

2 Karina Hansen<sup>1</sup>, Nanna B. Karlsson<sup>1,\*</sup>, Penelope How<sup>1</sup>, Ebbe Poulsen<sup>2</sup>, John  
3 Mortensen<sup>3</sup>, and Søren Rysgaard<sup>2</sup>

4 <sup>1</sup>Department of Glaciology and Climate, Geological Survey of Denmark and  
5 Greenland, Copenhagen, Denmark

6 <sup>2</sup>Arctic Research Centre, Department of Biology, Aarhus University, Aarhus,  
7 Denmark

8 <sup>3</sup>Greenland Climate Research Centre, Greenland Institute of Natural Resources,  
9 Nuuk, Greenland

10 \*nbk@geus.dk

## 11 **Abstract**

12 The interaction between glacier fronts and ocean waters is one of the key uncertainties for  
13 projecting future ice mass loss. Direct observations at glacier fronts are sparse, but studies  
14 indicate that the magnitude and timing of freshwater fluxes are crucial in determining fjord  
15 circulation, ice frontal melt and ecosystem habitability. In particular, wintertime dynamics  
16 are severely understudied due to inaccessible conditions, leading to a bias towards summer  
17 observations. Here, we present in-situ observations of temperature and salinity acquired in late  
18 winter in Greenland at the front of a marine-terminating glacier and in surrounding fjords.  
19 Our observations indicate the existence of an anomalously fresh pool of water by the glacier  
20 front, suggesting that meltwater generated at the bed of the glacier discharges during winter.  
21 The results suggest that warm Atlantic water and nutrients are entrained at the glacier front,  
22 leading to enhanced frontal melt and increased nutrient levels. Our findings have implications  
23 for understanding the heat exchange between glacier fronts and ocean waters, glacier frontal  
24 melt rates, ocean mixing and currents, and biological production.

## 25 *Main*

26 In Greenland, marine-terminating glaciers release meltwater at depth, causing a mixing of buoyant  
27 meltwater and saline ocean water [1, 2]. The discharge of subglacial meltwater and subsequent mixing  
28 leads to an upwelling of deep fjord waters close to the glacier fronts, influencing the circulation  
29 in the fjord systems [3, 4]. The meltwater impacts glacial frontal melt [5, 6] and ice mélange  
30 melt [7], thereby modifying the mass loss from marine-terminating glaciers and consequently glacier  
31 contribution to future sea-level rise [8, 9]. The upwelling also impacts the influx and mixing of

32 nutrients [10, 11, 12], enhancing biological primary productivity and providing feeding grounds for  
33 fish and seabirds [13, 14].

34 Greenland fjords experience large seasonal variability in temperature and salinity [4, 15]. During  
35 the summer, subglacial meltwater, predominantly from surface runoff, has been observed in fjord  
36 waters as a layered structure below the surface layer [7]. In contrast, winter measurements of  
37 subglacial discharge into Greenland fjords are effectively unprecedented. Thus, the volume of winter  
38 subglacial discharge and its impact on fjord systems remains an open question [16], and model  
39 estimates of winter meltwater differ by orders of magnitude [5, 17, 18]. Measurements in Kangarsuneq  
40 (in Nuup Kangerlua, West Greenland) revealed a considerable difference in temperature-salinity  
41 profiles between summer and winter, suggesting no noteworthy freshwater outflow from nearby  
42 glaciers during winter [1]. Studies of the Milne Fjord epishelf lake, northern Canada, report similar  
43 findings suggesting that winter freshwater discharge is negligible [19]. In contrast, studies from  
44 Svalbard fjords have found evidence of freshwater input during winter [20, 21] and early spring [22].  
45 However, due to the shallow fjord depths (10s of metres), and consequently shallow grounding lines  
46 [21, 22], this meltwater is likely added directly into the fjord surface layers, implying that its effect  
47 on fjord circulation is separate from subglacial freshwater discharged at depth (100s metres).

48 However, due to the shallow fjord depths, this meltwater is likely added directly into the fjord  
49 surface layers, implying that its effect on fjord circulation is separate from subglacial freshwater  
50 discharged at depth.

51 In contrast to observations, theoretical estimates of winter freshwater volumes indicate that sub-  
52 glacial meltwater discharges at depth into Greenland fjords all year round [17, 18, 23]. However,  
53 fjord circulation models disagree on the importance of winter discharge for heat and water exchange  
54 [24, 25]. In the absence of other freshwater fluxes, the winter discharge of glacial meltwater may  
55 have a pronounced influence on fjord dynamics, but its impact will depend on water volumes and  
56 fjord/glacier settings [16]. This underscores the complexity of bathymetry and heat exchange dy-  
57 namics between the shelf and marine-terminating glaciers within individual fjords. Finally, the  
58 fast-changing Arctic climate may already be causing shifts in wintertime conditions, highlighting  
59 the urgency for a better understanding of wintertime dynamics. To our knowledge, our study is the  
60 first to measure and document the existence of subglacial freshwater in a Greenland fjord during  
61 winter, shedding light on a hitherto undocumented process.

## 62 **In-situ observations of temperature and salinity**

63 During a dedicated field season in March 2023, we carried out in-situ observations of water properties  
64 at Eqalorutsit Kangilliit Sermiat (at times referred to as Qajuutaap) and neighbouring fjords (Fig. 1).  
65 Eqalorutsit Kangilliit Sermiat is one of the largest marine-terminating glaciers in South Greenland  
66 (its drainage basin and discharge rates are only matched by neighbouring Eqalorutsit Killiit Sermiat  
67 [26, 23]) with an ice front grounded several hundred metres below sea level and a grounding line  
68 depth that in places exceeds 400 m below sea level [27]. The glacier discharges into an eastern  
69 branch of Sermilik Fjord, which forms the inner part of Ikarsuaq Fjord (formerly Bredefjord). The  
70 fjord depth ranges from 60 m to 600 m below sea level, but bathymetric maps in the middle part of

71 the fjord are highly uncertain due to a lack of in-situ observations.

72 To retrieve temperature and salinity measurements, we developed and deployed a novel uncrewed  
73 aerial vehicle (UAV) solution (Fig. 2). Dense ice mélange has prevented previous studies from  
74 acquiring measurements in glacial fjords during winter, and the UAV was crucial to our success.  
75 The UAV platform consists of a modified kit helicopter with an onboard autonomous winch and  
76 a commercial CTD (conductivity, temperature, and depth) sensor payload (see [28] and methods).  
77 Its maximum total flight time is 24 minutes, allowing for measurements to be collected up to a  
78 distance of 6 km although our measurements were acquired less than 1.5 km from the deployment  
79 sites. We carried out additional CTD deployments in front of Eqalorutsit Kangilliit Sermiat, where  
80 flat, walkable fjord ice enabled us to drill two holes manually in the ice (Fig. 3). The heavy fjord-ice  
81 conditions in neighbouring Tunulliarfik Fjord also made it possible to drill a hole manually and make  
82 CTD casts.

83 Temperature and salinity data were derived from the CTD profiles, and salinity was calculated  
84 using the practical salinity scale (PSS-78). In the upper 30 m, temperature and salinity conditions  
85 cluster in three characteristic patterns (Fig. 4): the coldest and freshest conditions were found near  
86 the glacier front (St. 1 and 2, orange and red lines, respectively), transitioning to slightly warmer and  
87 saltier water in the ice mélange (St. 3, 4, 5, 6, rose, magenta, pink, and blue lines, respectively) and  
88 Sermilik fjord (St. 7, turquoise lines). Compared to these measurements, conditions in Tunulliarfik  
89 fjord (St. 8, yellow line) are warmer and saltier, indicating that coastal water modifies the fjord  
90 waters. Below 40 m depth, measurements closest to the glacier front (St. 1 and 2) reach salinity  
91 levels similar to those in Tunulliarfik fjord (St. 8). For context, we include summer measurements  
92 from the OMG (Oceans Melting Greenland) project [29, 30] and from the Greenland Institute of  
93 Natural Resources (GINR) (Fig. 4, brown lines).

94 In the  $T$ - $S$ -diagram (Fig. 4c), St. 1 and 2 measurements show a two-minima temperature profile  
95 (black arrows). Previous studies have interpreted two-minima temperature profiles as subglacial  
96 discharge [1, 7]. In contrast, two-minima temperature profiles are not seen in our CTD observations  
97 from the ice mélange (St. 3-6) or Sermilik fjord (St. 7). The down-fjord observations (St. 3-  
98 6) display a halocline layer (15-38 m depth) in the  $T$ - $S$ -diagram that follows a melt line with an  
99 observed slope of  $2.5^{\circ}\text{C}$  per salinity unit, which corresponds to the Gade-slope [31]. According to  
100 the Gade model [31], the mixing of melted glacial ice with seawater appears as a straight line in  
101 a  $T$ - $S$ -diagram with a slope of about  $2.5^{\circ}\text{C}$  per salinity unit. Thus, the down-fjord observations  
102 indicate that the freshening can be explained solely by the melting of ice mélange and stranded  
103 icebergs, while the freshening observed at St. 1 and 2 is caused by a mix of melt from ice mélange  
104 and icebergs, and subglacial discharge. Notably, measurements from St. 1 and 2 follow the same  
105  $T$ - $S$ -line as water in Tunulliarfik fjord (St. 8), indicating an influence from coastal water.

106 Fig. 4 also includes a rare winter observation from Nuup Kangerlua in West Greenland acquired  
107  $\sim 4$  km from the glacier front of Kangiata Nunaata Sermia (black line, referred to as GF10099  
108 [1]). A halocline layer (below 17 m depth) caused by melting of the ice mélange can be seen in our  
109 down-fjord observations (St. 3-8) and in GF10099. Comparison with our St. 1 and 2 measurements  
110 highlights the novelty of our observations. Where the surface layer temperature of GF10099 follows  
111 the freezing line, St. 1 and 2 profiles do not reach the freezing point and have local temperature

112 minima, showing a likely input of warmer waters such as a mixture of ambient deep fjord waters and  
113 subglacial meltwater discharge meltwater. Based on our observations, we suggest that 1) meltwater  
114 enters the fjord subglacially from Eqalorutsit Kangilliit Sermiat, freshening the surface layer and 2)  
115 the meltwater accumulates at the glacier front under the mélange in a “fresh surface pool of water”  
116 (Fig. 3) similar to reported epishelf lakes [19].

## 117 **Freshwater volumes and sources**

118 To our knowledge, our study is the first to document the existence of subglacial meltwater in a  
119 Greenland fjord during winter and to report evidence of upwelling at depth. The two-minima  
120 signal in our data is not as strong as observed during summer conditions (brown lines, Fig. 4, also  
121 [4]), indicating that the subglacial discharge may not be substantial. The fact that the freshwater  
122 pool is spatially confined is the likely reason why it has not been observed by previous studies, as  
123 measurements in those studies were retrieved 4 km [1] and 6 km [32] from the glacier front compared  
124 to our measurements that were 1 km (St. 1), 1.7 km (St. 2) and 5 km (St. 3) from the front.

125 Subglacial water may have different provenances. During summer, subglacially discharged water  
126 derives predominantly from surface meltwater that enters the subglacial system via moulins and  
127 crevasses [33]. During winter, in the absence of surface melt, the origin of the water is less clear. We  
128 suggest that the observed pool of meltwater originates from basal melting, that is, from melting at  
129 the interface between ice and bedrock. The basal conditions of the Greenland ice sheet are not well  
130 known, but estimates indicate that large parts of the ice sheet’s base are at the melting point [34].  
131 Studies suggest that basal melt is predominantly caused by heat from friction and geothermal flux  
132 [17, 35], and therefore, basal melt discharges during all seasons, making basal meltwater a potential  
133 source of wintertime freshwater.

134 Potential freshwater sources include surface melt and glacier-lake drainage events. Here, we  
135 outline why we discard these two meltwater sources as explanations for our measurements. Firstly,  
136 while large volumes of surface meltwater enter Sermilik Fjord in the summertime, the winter surface  
137 melt volume is orders of magnitude smaller due to low air temperatures (see Fig. S1). We estimate  
138 the likely surface melt using an improved Positive Degree Day model [36] and in-situ measurements  
139 from the PROMICE Automatic Weather Stations (AWS) [37] (see Fig. 1 and methods). Our results  
140 indicate that surface melt occurred for two days in early March (see Fig. S2). Only the lowest-  
141 elevation AWS experienced surface melt with daily melt rates of 5.6 mm and 6.4 mm on the 2nd and  
142 3rd of March, respectively (three weeks before our measurements began). Given the small volume of  
143 meltwater generated, we posit that the water is unlikely to have penetrated to the bed of the glacier  
144 and that the majority of the water was retained and refrozen close to the ice surface, either in the  
145 broken and weathered bare-ice surface or in snow pockets [38]. This is supported by observational  
146 evidence of refrozen ice, snow pockets and dry crevasses at the glacier margin (Fig. S3).

147 While we discard recent surface melt as a potential source of freshwater, a delayed release of surface  
148 meltwater generated during the previous melt season could contribute to the observed freshwater  
149 signal. The travel time of meltwater in the Greenland subglacial system is poorly constrained;  
150 however, numerous studies (as summarised in [39]) have found evidence that the subglacial system

151 drains highly efficiently, indicating an overall limited storage capacity. This is supported by a recent  
152 study that used measurements of shifts in the Greenland bedrock to estimate that the average water  
153 storage time in South Greenland is  $31 \pm 12$  days [40]. Local topography may further promote surface  
154 water storage by pooling water into subglacial lakes. For example, evidence of winter meltwater from  
155 a land-terminating glacier in Greenland [41] was found upstream of an area previously identified as  
156 a potential area for subglacial water storage [42]. However, no subglacial lakes have been identified  
157 in our study area [43]. Lacking isotope measurements, we cannot disentangle surface meltwater from  
158 basal meltwater and it is possible that our observations represent a mix of both meltwater sources.

159 A second freshwater source is the drainage of ice-marginal lakes. Thus, we investigated 21 lakes  
160 that share a margin with the glacier’s catchment area (mapped in 2017 [44]). Between January  
161 and April 2023, five of the 21 ice-marginal lakes around the lateral margins of Eqalorutsit Kangilliit  
162 Sermiat could be identified. Little is known about the dynamics of these lakes; however, satellite  
163 images suggest that their areas varied insignificantly during our period of interest and there is no  
164 evidence of glacial lake outburst floods or full drainage events during this period (see methods).

165 Other sources of freshwater at glacier fronts include melting of the glacier front itself. The  
166 frontal melt contribution to the freshwater budget of fjords is unresolved and recent laboratory  
167 studies suggest that frontal melt may be underestimated in models [45]. Nevertheless, observations  
168 in a Greenland fjord showed that the contribution from frontal melt is minor due to the small front  
169 surface compared to the ice mélange surface [7]. Importantly, meltwater originating from frontal  
170 melt will follow the Gade slope; therefore, if the freshwater signal consisted of frontal meltwater  
171 only, we would not observe a two-minima temperature profile.

172 Our study is the first to successfully measure meltwater linked to basal meltwater at a glacier  
173 front as opposed to precipitation or surface melt [20, 41]. The estimated monthly basal melt of  
174 Eqalorutsit Kangilliit Sermiat is  $3.8 \times 10^6 \text{ m}^3$  corresponding to 2 % of the glacier’s annual mass loss  
175 [23]. This estimate is highly uncertain, and we leverage our CTD observations to evaluate the amount  
176 of freshwater necessary to cause the observed freshening. Our results indicate a freshwater volume  
177 corresponding to  $2.4 \times 10^5 \text{ m}^3$  (see methods). This estimate includes all sources that contribute to  
178 freshening the water at the front, including meltwater from the glacier front and the delayed release  
179 of surface meltwater, and it should, therefore, be considered an upper bound. Nevertheless, our  
180 estimate is an order of magnitude lower than the theoretically estimated monthly basal melt. We  
181 suggest several reasons for this discrepancy that are not mutually exclusive. Firstly, the source area  
182 for the basal meltwater is reconstructed based on surface and bed topography, where the latter has  
183 uncertainties upwards of 300 m [27]. Therefore, the source area may be smaller than estimated,  
184 lowering the modelled basal meltwater volume discharging at the glacier front. Secondly, studies  
185 suggest that the subglacial system can shut down during winter [46], blocking the transport of basal  
186 meltwater from upstream parts of the glacier basin. This potential disconnection between parts of  
187 the subglacial system may be highly dependent on ice-flow velocities and the glacier’s topographic  
188 setting. Finally, our Station 1 and 2 measurements were acquired in a small bay a few kilometres  
189 east of where the glacier plume emerges in the summer. If it had been possible to get closer to the  
190 plume’s likely central outflow, we might have seen a stronger freshwater signal.

## 191 **Impacts of winter meltwater discharge**

192 Our measurements indicate that basal meltwater released subglacially during winter modifies near-  
193 glacier water properties and influences processes controlling ice/fjord interactions, fjord dynamics  
194 and ecosystems. Modelling studies of summer plumes [47] have shown that upwelling of Atlantic  
195 Water driven by plumes may substantially warm near-glacier waters at intermediate depth, affecting  
196 the distribution and magnitude of frontal melt. We suggest that winter discharge will have a similar  
197 effect, i.e., enhanced mixing and entrainment of ambient water at the glacial front. Ambient water  
198 temperatures above 0°C, typically from Atlantic Water, will accelerate frontal melting. Conversely,  
199 for glaciers terminating in water with ambient temperatures below 0°C, winter discharge may pro-  
200 mote refreezing and frazil ice formation in the fjord [48]. Thus, glaciers in contact with warmer  
201 waters, such as those in Southwest Greenland [49], are especially vulnerable to the effects of winter  
202 discharge, and an increase in winter freshwater would lead to increased frontal melt. However, there  
203 is a lack of understanding regarding the seasonal variation of water mass properties near glaciers  
204 and subglacial discharge outside the summer months [16], and more work is needed to include this  
205 effect in projections of future glacier mass loss from oceanic forcing, e.g., [9]. Thus, our findings  
206 underscore the urgent need to understand the role and impact of winter subglacial discharge on fjord  
207 dynamics.

208 The winter subglacial discharge from Eqaqorutsit Kangilliit Sermiat likely replenishes nutrients  
209 in the surface waters, thereby readying the system for expansive primary production during spring  
210 when the ice mélange breaks up. Hence, winter subglacial discharge in the inner parts of fjords  
211 may play a more critical role in priming the spring phytoplankton production than previously an-  
212 ticipated. It has been reported that the spring bloom in a marine-terminating glacier fjord will be  
213 triggered by out-fjord winds and coastal inflows driving an upwelling in the inner part of the fjord,  
214 hereby supplying nutrient-rich water to the surface layer [50]. Our observations suggest that winter  
215 subglacial discharge may entrain nutrients from deeper waters and accumulate them in a surface  
216 pool of water beneath the ice mélange near the glacier front. As a result, favourable conditions for  
217 a spring phytoplankton bloom are expected to establish when the mélange breaks up as observed  
218 further north in the Nuup Kangerlua fjord system [51]. It is noteworthy that the spring bloom  
219 might not occur directly in front of the glacier but further out in the fjord, as the nutrient pool  
220 will track the drifting ice pushed by prevailing winds from the northeast during spring (see observed  
221 wind directions in Fig. S6). This further underscores the seasonal significance of marine-terminating  
222 glaciers in stimulating primary production.

223 Observations and models suggest that subglacial discharge causes fjord circulation patterns lead-  
224 ing to a renewal of fjord basin waters over seasonal time scales [2, 52]. Although melt from icebergs  
225 and ice mélange probably dominates the winter freshwater budget for most ice-filled fjords [53], any  
226 inflow of glacial freshwater may be of physical and biogeochemical significance [16]. Nevertheless,  
227 most fjord circulation models focus on summertime dynamics aiming to understand processes occur-  
228 ring during the peak meltwater season [54, 55]. In the near future, increasing Arctic temperatures  
229 are likely to lead to a speed-up of Greenland glaciers [56] and consequently an increase in basally  
230 generated meltwater due to increased friction [35] and thereby also an increased winter freshwater

231 discharge. Thus, there is an urgent need to understand the role and impact of winter subglacial  
232 discharge on fjord dynamics.

233 Our unique observations of winter subglacial discharge highlight the importance of this severely  
234 understudied freshwater source and demonstrate the potential of UAV-supported observations during  
235 the Arctic winter. The potentially disproportionately large influence of winter subglacial discharge  
236 on fjord waters when considering its comparatively small volume, coupled with its ability to enhance  
237 spring primary production, emphasises the significant impact marine-terminating glaciers can exert  
238 on fjord waters, fjord circulation, and ecosystem productivity, with consequences for fisheries in the  
239 coastal zone surrounding Greenland.

## 240 **Acknowledgements**

241 This work was supported by a Villum Experiment project to NBK from the Villum Foundation  
242 (project no. 40858). Further support was provided by PROMICE, funded by the Geological Sur-  
243 vey of Denmark and Greenland (GEUS) and the Danish Ministry of Climate, Energy and Utilities  
244 under the Danish Cooperation for Environment in the Arctic (DANCEA), conducted in collab-  
245 oration with DTU Space (Technical University of Denmark) and Asiaq Greenland Survey. The  
246 development of the UAV was supported by Aage V Jensens Foundations to the project "Green-  
247 land gradients Flagship project". PH was supported by a European Space Agency Living Planet  
248 Fellowship (4000136382/21/I-DT-lr) entitled "Examining Greenland's Ice Marginal Lakes under a  
249 Changing Climate". We thank Baptiste Vandecrux (GEUS) for advice and insightful discussions on  
250 calculating surface melt. The skilled and patient employees of the Department of Biology mechanical  
251 and electrical workshops are acknowledged for their significant contributions during the design and  
252 build of the ARC-AWS. We acknowledge the helpful community of ArduPilot and Bill Geyer for  
253 support and guidance during UAV development. Egon R. Frandsen is acknowledged for logistical  
254 support during fieldwork. We thank the pilots from SERMEQ helicopters for their support and  
255 enthusiasm during the 2023 fieldwork.

## 256 **Author contributions statement**

257 NBK conceived of the study in collaboration with SR. KH managed the project and planned the  
258 fieldwork campaign. EP developed the UAV solution with input from SR. EP, SR, KH and NBK  
259 collected the data and analysed it with input from JM. KH calculated surface melt rates. PH  
260 compiled and analysed the ice-marginal lake observations. NBK, SR and KH led the writing of the  
261 article with contributions from all authors. NBK and SR acquired the funding for the work. All  
262 authors reviewed the manuscript.

## 263 **Competing interests**

264 The authors declare that they have no competing interests.



## Figure captions

Figure 1: *Overview map of our study area and measurement sites. The locations of our measurement stations are indicated with coloured circles, where measurements acquired by our Uncrewed Autonomous Vehicle (UAV) are outlined with a thick black line. Measurements from the OMG project (Oceans Melting Greenland [30]) and the Greenland Institute of Natural Resources (GINR, KR23034) are indicated with a brown diamond and brown triangle, respectively. PROMICE (Programme for Monitoring of the Greenland Ice Sheet) automatic weather stations (AWS) are marked with black stars. Ice marginal lakes are outlined with turquoise [44], and the ice sheet is coloured grey with 200 m surface topography contours in dashed grey lines from [27, 57]. The background image is optical satellite data from Sentinel 2 (Copernicus Sentinel data, processed by the European Space Agency) from the 27th of March 2023. The location of the map is indicated on the overview map in red, also showing 500 m surface topography contours [27, 57] and surface velocities in blue [58].*

Figure 2: *Photographs of our UAV platform. (a) Complete UAV platform with CTD payload extended. (b) UAV during profiling in a narrow section of open water created by a seal. The seal hole in the sea ice is smaller (approximately 0.5 m) than the flooded surface area. Note the line extending from the UAV to the submerged CTD instrument. The UAV platform has a length of 1.145 m and a rotor diameter of 1.455 m. Photos are from two different deployments, courtesy of Lars Ostenfeld and the authors.*

Figure 3: *Schematic of the measurement conditions for the UAV and the manual drill in glacier/ice melange/fjord system. (a) and (b) show enlarged versions of our measurement techniques.*

Figure 4: *In-situ measurements from the CTD sensors. The figures show CTD profiles of (a) temperature and (b) salinity, and (c) the corresponding T-S-diagram (locations are shown in Fig. 1). Observations from GINR (KR23034, July 2023) and the OMG project (August 2018) are shown as brown lines. Dotted lines indicate measurements from neighbouring Tunulliarfik fjord. A GINR winter observation from Nuup Kangerlua in West Greenland is shown in black (GF10099, April 2010). A Gade-slope of  $2.5^{\circ}\text{C}$  per salinity unit is indicated with thick grey. The freezing point line of seawater is shown as a dashed-dotted grey line. Black arrows indicate the two-temperature minima seen in St. 1 and 2 data.*

## References

- [1] Mortensen, J., Bendtsen, J., Motyka, R. J., Lennert, K., Truffer, M., Fahnestock, M. & Rysgaard, S. On the seasonal freshwater stratification in the proximity of fast-flowing tidewater outlet glaciers in a sub-Arctic sill fjord. *Journal of Geophysical Research: Oceans* **118**, 1382–1395 (2013).
- [2] Carroll, D., Sutherland, D. A., Shroyer, E. L., Nash, J. D., Catania, G. A. & Stearns, L. A. Modeling Turbulent Subglacial Meltwater Plumes: Implications for Fjord-Scale Buoyancy-Driven Circulation. *Journal of Physical Oceanography* 2169–2185 (2015).
- [3] Straneo, F. & Cenedese, C. The Dynamics of Greenland’s Glacial Fjords and Their Role in Climate. *Annual Review of Marine Science* **7**, 89–112 (2015).
- [4] Mortensen, J., Bendtsen, J., Lennert, K. & Rysgaard, S. Seasonal variability of the circulation system in a west Greenland tidewater outlet glacier fjord, Godthåbsfjord (64 N). *Journal of Geophysical Research: Earth Surface* **119**, 2591–2603 (2014).
- [5] Rignot, E., Xu, Y., Menemenlis, D., Mouginot, J., Scheuchl, B., Li, X., Morlighem, M., Seroussi, H., den Broeke, M. v., Fenty, I. *et al.* Modeling of ocean-induced ice melt rates of five west Greenland glaciers over the past two decades. *Geophysical Research Letters* **43**, 6374–6382 (2016).
- [6] Jackson, R., Nash, J., Kienholz, C., Sutherland, D., Amundson, J., Motyka, R., Winters, D., Skyllingstad, E. & Pettit, E. Meltwater intrusions reveal mechanisms for rapid submarine melt at a tidewater glacier. *Geophysical Research Letters* **47**, e2019GL085335 (2020).
- [7] Mortensen, J., Rysgaard, S., Bendtsen, J., Lennert, K., Kanzow, T., Lund, H. & Meire, L. Subglacial discharge and its down-fjord transformation in West Greenland fjords with an ice mélange. *Journal of Geophysical Research: Oceans* **125**, e2020JC016301 (2020).
- [8] Beckmann, J., Perrette, M., Beyer, S., Calov, R., Willeit, M. & Ganopolski, A. Modeling the response of Greenland outlet glaciers to global warming using a coupled flow line–plume model. *The Cryosphere* **13**, 2281–2301 (2019). URL <https://www.the-cryosphere.net/13/2281/2019/>.
- [9] Slater, D. A., Felikson, D., Straneo, F., Goelzer, H., Little, C. M., Morlighem, M., Fettweis, X. & Nowicki, S. Twenty-first century ocean forcing of the Greenland ice sheet for modelling of sea level contribution. *The Cryosphere* **14**, 985–1008 (2020).
- [10] Meire, L., Mortensen, J., Meire, P., Juul-Pedersen, T., Sejr, M. K., Rysgaard, S., Nygaard, R., Huybrechts, P. & Meysman, F. J. Marine-terminating glaciers sustain high productivity in Greenland fjords. *Global Change Biology* **23**, 5344–5357 (2017).
- [11] Kanna, N., Sugiyama, S., Ohashi, Y., Sakakibara, D., Fukamachi, Y. & Nomura, D. Upwelling of Macronutrients and Dissolved Inorganic Carbon by a Subglacial Freshwater Driven Plume

- 301 in Bowdoin Fjord, Northwestern Greenland. *Journal of Geophysical Research: Biogeosciences*  
302 **123**, 1666–1682 (2018).
- 303 [12] Hopwood, M. J., Carroll, D., Dunse, T., Hodson, A., Holding, J. M., Iriarte, J. L., Ribeiro, S.,  
304 Achterberg, E. P., Cantoni, C., Carlson, D. F., Chierici, M., Clarke, J. S., Cozzi, S., Fransson,  
305 A., Juul-Pedersen, T., Winding, M. H. & Meire, L. Review article: How does glacier discharge  
306 affect marine biogeochemistry and primary production in the Arctic? *Cryosphere* **14**, 1347–1383  
307 (2020).
- 308 [13] Hopwood, M. J., Carroll, D., Browning, T. J., Meire, L., Mortensen, J., Krisch, S. & Achterberg,  
309 E. P. Non-linear response of summertime marine productivity to increased meltwater discharge  
310 around Greenland. *Nature Communications* **9** (2018).
- 311 [14] Nishizawa, B., Kanna, N., Abe, Y., Ohashi, Y., Sakakibara, D., Asaji, I., Sugiyama, S., Ya-  
312 maguchi, A. & Watanuki, Y. Contrasting assemblages of seabirds in the subglacial melt-  
313 water plume and oceanic water of Bowdoin Fjord, northwestern Greenland. *ICES Journal*  
314 *of Marine Science* **77**, 711–720 (2019). URL <https://doi.org/10.1093/icesjms/fsz213>.  
315 <https://academic.oup.com/icesjms/article-pdf/77/2/711/32881925/fsz213.pdf>.
- 316 [15] Jackson, R. H., Straneo, F. & Sutherland, D. A. Externally forced fluctuations in ocean tem-  
317 perature at Greenland glaciers in non-summer months. *Nature Geoscience* **7**, 503–508 (2014).
- 318 [16] Vonnahme, T. R., Nowak, A., Hopwood, M. J., Meire, L., Sogaard, D. H., Krawczyk, D.,  
319 Kalhagen, K. & Juul-Pedersen, T. Impact of winter freshwater from tidewater glaciers on fjords  
320 in Svalbard and Greenland; A review. *Progress in Oceanography* **219**, 103144 (2023). URL  
321 <https://www.sciencedirect.com/science/article/pii/S0079661123001878>.
- 322 [17] Cook, S. J., Swift, D. A., Kirkbride, M. P., Knight, P. G. & Waller, R. I. The empirical basis  
323 for modelling glacial erosion rates. *Nature Communications* **11** (2020).
- 324 [18] Sommers, A., Meyer, C., Morlighem, M., Rajaram, H., Poinar, K., Chu, W. & Mejia, J. Sub-  
325 glacial hydrology modeling predicts high winter water pressure and spatially variable transmis-  
326 sivity at Helheim Glacier, Greenland. *Journal of Glaciology* 1–13 (2023).
- 327 [19] Hamilton, A. K., Mueller, D. & Laval, B. E. Ocean Modification and Seasonality in a Northern  
328 Ellesmere Island Glacial Fjord Prior to Ice Shelf Breakup: Milne Fiord. *Journal of Geophysical*  
329 *Research: Oceans* **126**, e2020JC016975 (2021). E2020JC016975 2020JC016975.
- 330 [20] Fransson, A., Chierici, M., Nomura, D., Granskog, M. A., Kristiansen, S., Martma, T. &  
331 Nehrke, G. Effect of glacial drainage water on the CO<sub>2</sub> system and ocean acidification state in  
332 an Arctic tidewater-glacier fjord during two contrasting years. *Journal of Geophysical Research:*  
333 *Oceans* **120**, 2413–2429 (2015).
- 334 [21] Marchenko, A. V., Morozov, E. G. & Marchenko, N. A. Supercooling of Seawater Near the  
335 Glacier Front in a Fjord. *Earth Science Research* **6**, 97–108 (2017).

- 336 [22] Vonnahme, T. R., Persson, E., Dietrich, U., Hejdukova, E., Dybwad, C., Elster, J., Chierici, M.  
337 & Gradinger, R. Early spring subglacial discharge plumes fuel under-ice primary production at  
338 a Svalbard tidewater glacier. *The Cryosphere* **15**, 2083–2107 (2021).
- 339 [23] Karlsson, N. B., Mankoff, K. D., Solgaard, A. M., Larsen, S. H., How, P. R., Fausto, R. S.  
340 & Sørensen, L. S. A data set of monthly freshwater fluxes from the Greenland ice sheet’s  
341 marine-terminating glaciers on a glacier–basin scale 2010–2020. *GEUS Bulletin* **53** (2023).  
342 URL <https://geusbulletin.org/index.php/geusb/article/view/8338>.
- 343 [24] Fraser, N. J., Inall, M. E., Magaldi, M. G., Haine, T. W. N. & Jones, S. C. Wintertime  
344 Fjord-Shelf Interaction and Ice Sheet Melting in Southeast Greenland. *Journal of Geophysical*  
345 *Research: Oceans* **123**, 9156–9177 (2018).
- 346 [25] Hager, A. O., Sutherland, D. A. & Slater, D. A. Local forcing mechanisms challenge parameter-  
347 izations of ocean thermal forcing for Greenland tidewater glaciers. *The Cryosphere* **18**, 911–932  
348 (2024).
- 349 [26] Mankoff, K. D., Noël, B., Fettweis, X., Ahlstrøm, A. P., Colgan, W., Kondo, K., Langley, K.,  
350 Sugiyama, S., van As, D. & Fausto, R. S. Greenland liquid water discharge from 1958 through  
351 2019. *Earth System Science Data* **12**, 2811–2841 (2020).
- 352 [27] Morlighem, M., Williams, C. N., Rignot, E., An, L., Arndt, J. E., Bamber, J. L., Catania, G.,  
353 Chauché, N., Dowdeswell, J. A., Dorschel, B., Fenty, I., Hogan, K., Howat, I., Hubbard, A.,  
354 Jakobsson, M., Jordan, T. M., Kjeldsen, K. K., Millan, R., Mayer, L., Mouginot, J., Noël, B.  
355 P. Y., O’Cofaigh, C., Palmer, S., Rysgaard, S., Seroussi, H., Siegert, M. J., Slabon, P., Straneo,  
356 F., van den Broeke, M. R., Weinrebe, W., Wood, M. & Zinglensen, K. B. BedMachine v3:  
357 Complete Bed Topography and Ocean Bathymetry Mapping of Greenland From Multibeam  
358 Echo Sounding Combined With Mass Conservation. *Geophysical Research Letters* **44**, 11,051–  
359 11,061 (2017).
- 360 [28] Poulsen, E., Rysgaard, S., Hansen, K. & Karlsson, N. B. Uncrewed aerial vehicle with on-  
361 board winch system for rapid, cost-effective, and safe oceanographic profiling in hazardous and  
362 inaccessible areas. *HardwareX* **18**, e00518 (2024).
- 363 [29] OMG. 2020. OMG CTD Conductivity Temperature Depth. Ver. 1. Dataset accessed [2023-12-  
364 18].
- 365 [30] Fenty, I., Willis, J. K., Khazendar, A., Dinardo, S., Forsberg, R., Fukumori, I., Holland, D.,  
366 Jakobsson, M., Moller, D., Morison, J. *et al.* Oceans Melting Greenland: Early results from  
367 NASA’s ocean-ice mission in Greenland. *Oceanography* **29**, 72–83 (2016).
- 368 [31] Gade, H. G. Melting of Ice in Sea Water: A Primitive Model with Application to the Antarctic  
369 Ice Shelf and Icebergs. *Journal of Physical Oceanography* **9**, 189 – 198 (1979).
- 370 [32] Straneo, F., Curry, R. G., Sutherland, D. A., Hamilton, G. S., Cenedese, C., Våge, K. &  
371 Stearns, L. A. Impact of fjord dynamics and glacial runoff on the circulation near Helheim  
372 Glacier. *Nature Geoscience* **4**, 322–327 (2011).

- 373 [33] Hoffman, M. J., Andrews, L. C., Price, S. F., Catania, G. A., Neumann, T. A., Lüthi, M. P.,  
374 Gulley, J., Ryser, C., Hawley, R. L. & Morriss, B. Greenland subglacial drainage evolution  
375 regulated by weakly connected regions of the bed. *Nature Communications* **9** (2016).
- 376 [34] MacGregor, J. A., Chu, W., Colgan, W. T., Fahnestock, M. A., Felikson, D., Karlsson, N. B.,  
377 Nowicki, S. M. J. & Studinger, M. GBaTSv2: a revised synthesis of the likely basal thermal  
378 state of the Greenland Ice Sheet. *The Cryosphere* **16**, 3033–3049 (2022).
- 379 [35] Karlsson, N. B., Solgaard, A. M., Mankoff, K. D., Gillet-Chaulet, F., MacGregor, J. A., Box,  
380 J. E., Citterio, M., Colgan, W. T., Larsen, S. H., Kjeldsen, K. K., Korsgaard, N. J., Benn,  
381 D. I., Hewitt, I. J. & Fausto, R. S. A first constraint on basal melt-water production of the  
382 Greenland ice sheet. *Nature Communications* **12** (2021).
- 383 [36] Tsai, V. C. & Ruan, X. A simple physics-based improvement to the positive degree day model.  
384 *Journal of Glaciology* **64**, 661–668 (2018).
- 385 [37] Fausto, R., Mernild, S., Hasholt, B., Ahlstrøm, A. & Knudsen, N. Modeling suspended sediment  
386 concentration and transport, Mittivakkat glacier, southeast Greenland. *Arctic, Antarctic, and*  
387 *Alpine Research* **44**, 306–318 (2012).
- 388 [38] Cooper, M. G., Smith, L. C., Rennermalm, A. K., Miège, C., Pitcher, L. H., Ryan,  
389 J. C., Yang, K. & Cooley, S. W. Meltwater storage in low-density near-surface bare ice  
390 in the Greenland ice sheet ablation zone. *The Cryosphere* **12**, 955–970 (2018). URL  
391 <https://tc.copernicus.org/articles/12/955/2018/>.
- 392 [39] Nienow, P. W., Sole, A. J., Slater, D. A. & Cowton, T. R. Recent Advances in Our Under-  
393 standing of the Role of Meltwater in the Greenland Ice Sheet System. *Current Climate Change*  
394 *Reports* **3**, 330–344 (2017).
- 395 [40] Ran, J., Ditmar, P., van den Broeke, M. R., Liu, L., Klees, R., Khan, S. A., Moon, T., Li, J.,  
396 Bevis, M., Zhong, M., Fettweis, X., Liu, J., Noël, B., Shum, C. K., Chen, J., Jiang, L. & van  
397 Dam, T. Vertical bedrock shifts reveal summer water storage in Greenland ice sheet. *Nature*  
398 **635**, 108–113 (2024).
- 399 [41] Pitcher, L. H., Smith, L. C., Gleason, C. J., Miège, C., Ryan, J. C., Hagedorn, B., van As,  
400 D., Chu, W. & Forster, R. R. Direct Observation of Winter Meltwater Drainage From the  
401 Greenland Ice Sheet. *Geophysical Research Letters* **47**, e2019GL086521 (2020).
- 402 [42] Chu, W., Schroeder, D. M., Seroussi, H., Creyts, T. T., Palmer, S. J. & Bell, R. E. Extensive  
403 winter subglacial water storage beneath the Greenland Ice Sheet. *Geophysical Research Letters*  
404 **43**, 12,484–12,492 (2016).
- 405 [43] Livingstone, S. J., Li, Y., Rutishauser, A., Sanderson, R. J., Winter, K., Mikucki, J. A.,  
406 Björnsson, H., Bowling, J. S., Chu, W., Dow, C. F., Fricker, H. A., McMillan, M., Ng, F.  
407 S. L., Ross, N., Siegert, M. J., Siegfried, M. & Sole, A. J. Subglacial lakes and their changing  
408 role in a warming climate. *Nature Reviews Earth & Environment* **3**, 106–124 (2022).

- 409 [44] How, P., Messerli, A., Mätzler, E., Santoro, M., Wiesmann, A., Caduff, R., Langley, K., Bojesen,  
410 M. H., Paul, F., Kääb, A. *et al.* Greenland-wide inventory of ice marginal lakes using a multi-  
411 method approach. *Scientific reports* **11**, 4481 (2021).
- 412 [45] Wengrove, M. E., Pettit, E. C., Nash, J. D., Jackson, R. H. & Skillingstad, E. D. Melting of  
413 glacier ice enhanced by bursting air bubbles. *Nature Geoscience* **16**, 871–876 (2014).
- 414 [46] Flowers, G. E. Hydrology and the future of the Greenland Ice Sheet. *Nature Communications*  
415 **9** (2018).
- 416 [47] Cowton, T. R., Slater, D. A. & Inall, M. E. Subglacial-Discharge Plumes Drive Widespread  
417 Subsurface Warming in Northwest Greenland’s Fjords. *Geophysical Research Letters* **50**,  
418 e2023GL103801 (2023).
- 419 [48] Rooijakkers, F. J., Poulsen, E., Ruiz-Castillo, E. & Rysgaard, S. Evidence  
420 suggesting frazil ice crystal formation at the front of Hisinger Glacier in Dick-  
421 son Fjord, Northeast Greenland. *EGUsphere* **2024**, 1–20 (2024). URL  
422 <https://egusphere.copernicus.org/preprints/2024/egusphere-2024-2168/>.
- 423 [49] Rysgaard, S., Boone, W., Carlson, D., Sejr, M. K., Bendtsen, J., Juul-Pedersen, T., Lund, H.,  
424 Meire, L. & Mortensen, J. An Updated View on Water Masses on the pan-West Greenland  
425 Continental Shelf and Their Link to Proglacial Fjords. *Journal of Geophysical Research: Oceans*  
426 **125**, e2019JC015564 (2020).
- 427 [50] Meire, L., Mortensen, J., Rysgaard, S., Bendtsen, J., Boone, W., Meire, P. & Meysman, F. J.  
428 Spring bloom dynamics in a subarctic fjord influenced by tidewater outlet glaciers (Godthåbs-  
429 fjord, SW Greenland). *Journal of Geophysical Research: Biogeosciences* **121**, 1581–1592 (2016).
- 430 [51] Meire, L., Paulsen, M. L., Meire, P., Rysgaard, S., Hopwood, M. J., Sejr, M. K., Stuart-Lee,  
431 A., Sabbe, K., Stock, W. & Mortensen, J. Glacier retreat alters downstream fjord ecosystem  
432 structure and function in Greenland. *Nature Geoscience* (2023).
- 433 [52] Carroll, D., Sutherland, D. A., Shroyer, E. L., Nash, J. D., Catania, G. A. & Stearns, L. A.  
434 Subglacial discharge-driven renewal of tidewater glacier fjords. *Journal of Geophysical Research: Oceans*  
435 **122**, 6611–6629 (2017).
- 436 [53] Moon, T., Sutherland, D. A., Carroll, D., Felikson, D., Kehrl, L. & Straneo, F. Subsurface  
437 iceberg melt key to Greenland fjord freshwater budget. *Nature Geoscience* **11** (2018).
- 438 [54] Cape, M. R., Straneo, F., Beaird, N., Bundy, R. M. & Charette, M. A. Nutrient release to  
439 oceans from buoyancy-driven upwelling at Greenland tidewater glaciers. *Nature Geoscience* **12**  
440 (2019).
- 441 [55] Torsvik, T., Albretsen, J., Sundfjord, A., Kohler, J., Sandvik, A. D., Skarðhamar, J., Lindbäck,  
442 K. & Everett, A. Impact of tidewater glacier retreat on the fjord system: Modeling present  
443 and future circulation in Kongsfjorden, Svalbard. *Estuarine, Coastal and Shelf Science* **220**,  
444 152–165 (2019).

- 445 [56] Goelzer, H., Nowicki, S., Payne, A., Larour, E., Seroussi, H., Lipscomb, W. H., Gregory, J.,  
446 Abe-Ouchi, A., Shepherd, A., Simon, E., Agosta, C., Alexander, P., Aschwanden, A., Barthel,  
447 A., Calov, R., Chambers, C., Choi, Y., Cuzzone, J., Dumas, C., Edwards, T., Felikson, D.,  
448 Fettweis, X., Golledge, N. R., Greve, R., Humbert, A., Huybrechts, P., Clec'H, S. L., Lee, V.,  
449 Leguy, G., Little, C., Lowry, D., Morlighem, M., Nias, I., Quiquet, A., Rückamp, M., Schlegel,  
450 N. J., Slater, D. A., Smith, R., Straneo, F., Tarasov, L., Wal, R. V. D. & Broeke, M. V. D.  
451 The future sea-level contribution of the Greenland ice sheet: A multi-model ensemble study of  
452 ISMIP6. *Cryosphere* **14**, 3071–3096 (2020).
- 453 [57] Morlighem, M. e. a. IceBridge BedMachine Greenland, Version 5 (2022). URL  
454 <https://nsidc.org/data/IDBMG4/versions/5>.
- 455 [58] Solgaard, A., Kusk, A., Merryman Boncori, J. P., Dall, J., Mankoff, K. D., Ahlstrøm, A. P.,  
456 Andersen, S. B., Citterio, M., Karlsson, N. B., Kjeldsen, K. K., Korsgaard, N. J., Larsen, S. H.  
457 & Fausto, R. S. Greenland ice velocity maps from the PROMICE project. *Earth System Science*  
458 *Data* **13**, 3491–3512 (2021).



## 459 **Methods**

### 460 **UAV technology**

461 Crewed aircraft have been used previously to study fjord conditions by employing expendable CTD  
462 (also referred to as XCTD) instruments [30, 7, 32]. However, the method is constrained by aircraft  
463 hire and equipment replacement, as well as the fact that precise deployment within narrow openings  
464 in fjord ice is challenging. To alleviate these issues, we developed a novel UAV solution (Fig. 2). A  
465 complete description of the UAV, including hardware description, cost overview, and assembly and  
466 deployment instructions, is available in [28].

467 The UAV is based on a modified Align Trex 650X kit helicopter with an autopilot system and a  
468 custom payload attached. The autopilot provides autonomous flight capabilities and pilot assistance  
469 when manually operating the UAV. The UAV payload consists of a SonTek CastAway CTD sensor,  
470 a winch unit, and an HD camera attached to a gimbal. The Herelink HD Video system handles  
471 control, telemetry, and video transmission and has a tested range of 6 km. The winch unit consists of  
472 a winch motor that reels the CTD in and out and a pivot mechanism. This mechanism transitions  
473 the sensor from horizontal during takeoff, cruise, and landing to vertical during profiling. Once  
474 vertical, the winch motor lowers the CTD. A range of servo motors is used to control the pivot  
475 mechanism and gimbal and to engage and disengage the winch motor for the different stages of  
476 operation. The maximum measurement depth is 100 m, and a complete CTD profile (downcast and  
477 upcast) takes less than 10 minutes. The complete system is powered by a 22.2 V 14 Ah lithium  
478 polymer battery pack, which is insulated and preheated before deployment to improve performance  
479 in cold environments.

480 The takeoff weight of the complete UAV platform is 6.5 kg with a length of 1.145 m and a rotor  
481 diameter of 1.455 m. The maximum tested cruise speed is 16 m s<sup>-1</sup>. The UAV has been tested in  
482 wind speeds of up to 7 m/s with minimal effect on performance. All components, including batteries,  
483 controller, and CTD payload, can be packed in a 1.400x450x250 mm Zarges box for shipping and  
484 handling. During fieldwork, the UAV was transported inside the cabin of an AS350 helicopter, which  
485 had two crew members and three passengers. The total cost of the UAV platform with the CTD  
486 sensor is €13,000.

### 487 **Basal melt estimate**

488 The basal melt estimate presented here stems from already published data [23] based on methods  
489 developed in [35]. We briefly summarise the methods here and refer readers to the original study  
490 for more details. The basal melt rates  $b_m$  are derived from estimates of available heat sources ( $E$ )

$$b_m = E/(\rho L)$$

491 Where  $\rho$  is ice density, and  $L$  is the latent heat of fusion. In the absence of surface melt, the basal  
492 meltwater is generated by friction heat and the geothermal flux [35]. Using subglacial drainage catch-  
493 ments delineated by the hydropotential gradients [59] (calculated from surface and bed topography  
494 from BedMachine v5 [27]), the basal melt is routed to the front of the glacier. Results show that the

495 average monthly basal melt volume in March is  $3.8 \times 10^6 \text{ m}^3$  (2010-2020 averages) [23]. This assumes  
 496 that all melt generated at the bed is immediately transported to the front of the glacier and does  
 497 not account for the possibility of subglacial storage or delays in subglacial transport efficiency. The  
 498 uncertainty of the estimated basal melt is 21%, which stems from the fact that the basal conditions  
 499 of the Greenland ice sheet are widely unknown. The uncertainty encompasses the poorly constrained  
 500 geothermal flux, the frictional heat derived from ice-flow models using simplifying assumptions, and  
 501 the unknown subglacial water routing (see [35]). In Fig. S1, we compare the basal meltwater volume  
 502 to the surface meltwater volume. The uncertainty of surface meltwater estimate is 15%. It relates  
 503 to the inherent uncertainty in the regional climate model but also to the uncertainty in the delay  
 504 between meltwater production on the ice sheet and the discharge of the water at the margin, and  
 505 the delineation of drainage basins that determines the water routing (see [26] for details).

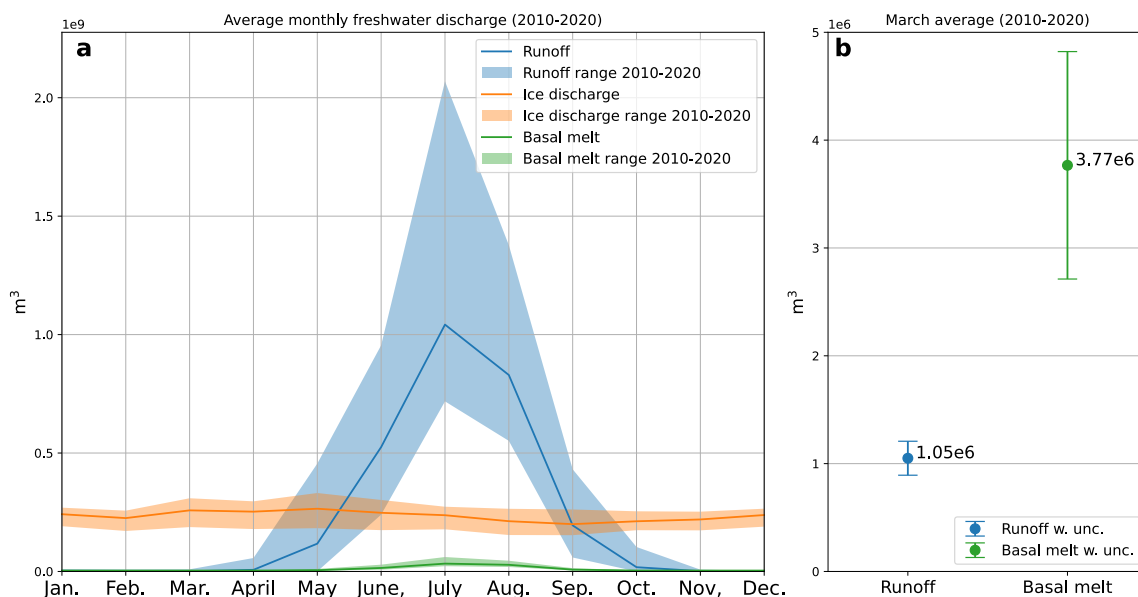


Figure S1: Average monthly freshwater fluxes for Eqalorutsit Kangilliit Sermiat 2010-2020 [23]. In (a) the shaded areas indicate the range of values from 2010-2020. In (b) error bars show the uncertainty associated with the average values for runoff and basal melt for March.

## 506 Estimates of surface runoff

507 The winter surface melt at elevations 280 m, 600 m and 900 m was estimated using an improved  
 508 Positive Degree Day (PDD) model that accounts for the time lag in the melt that occurs when the  
 509 air temperature is above  $0^\circ\text{C}$  while the temperature of the ice surface is not yet at the melting  
 510 point [36]. We combine the model with measurements from the PROMICE AWSs QAS<sub>L</sub>, QAS<sub>M</sub>  
 511 and QAS<sub>U</sub> [37, 60] (see Fig. 1). The improved PDD model uses ice surface temperatures to estimate  
 512 surface melt rates. Here, we input measured ice surface temperatures from the AWSs, when mea-  
 513 surements are available, or 2 m air temperatures, if ice surface temperatures are unavailable. During  
 514 the period of interest, air and ice surface temperature measurements are available from the AWSs at

515 280 m and 900 m elevation. There are no ice surface temperature measurements from the AWS at  
 516 600 m elevation, so we estimate the ice surface temperature using measured air temperatures from  
 517 the same AWS. We use a simple linear regression model trained on earlier measurements of air and  
 518 ice surface temperature. A simple validation of the linear regression model indicates that the linear  
 519 regression performs well with a Mean Squared Error of  $1.16^{\circ}\text{C}$  and an R-squared value of 0.97.  
 520 The AWS are situated 80km west of our study area. We investigate how representative the AWS  
 521 measurements are for our site by analysing the output from the Copernicus Arctic Regional Reanaly-  
 522 sis (CARRA) model [61]. In the Supplementary Materials, figures show the 2-metre air temperatures  
 523 from CARRA on a three-hour basis retrieved at grid points close to the AWS and from three elevation  
 524 ranges on Eqalorutsit Kangilliit Sermiat as shown on the maps. Also shown are the temperatures  
 525 from the AWS QAS<sub>L</sub>, QAS<sub>M</sub> and QAS<sub>U</sub> on daily and hourly resolution. As seen in the figures, the  
 526 CARRA air temperatures agree between the two sites, with a slight tendency for faster air cooling  
 527 at Sermilik Bræ between the 4th and 5th of March. We note that due to the spatial resolution of  
 528 2.5 km of the CARRA output, the elevations of the CARRA grid points do not necessarily represent  
 529 the exact altitude which will influence the temperature. We also note that the AWSs generally mea-  
 530 sure lower temperatures than CARRA predicts. Finally, surface runoff estimates from CARRA (not  
 531 shown) indicate zero surface runoff despite the warmer model temperatures. This gives us further  
 532 confidence that we are not underestimating the surface runoff using the improved PDD model.

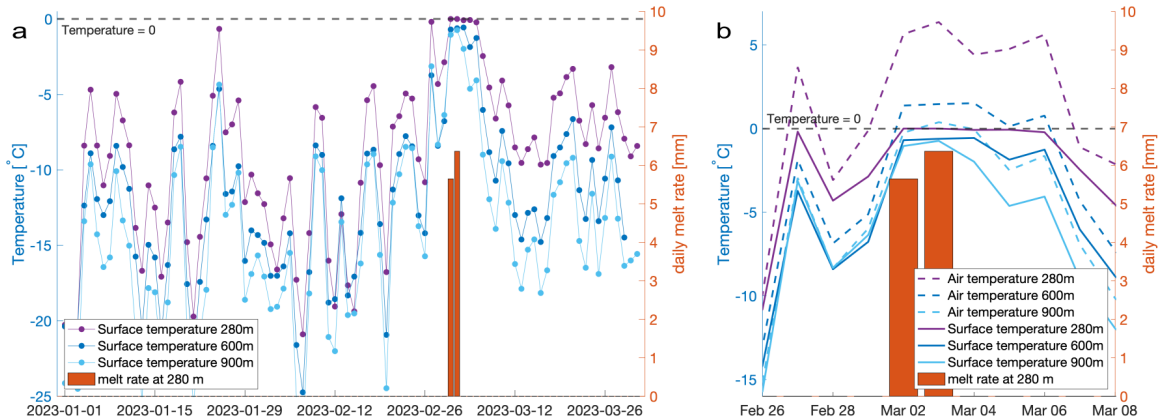


Figure S2: *Temperature time series at elevations 280 m, 600 m and 900 m by AWS approx. 80 km west of Eqalorutsit Kangilliit Sermiat and the modelled daily melt rate [36]. (a) Time series from 2023-01-01 to 2023-04-01 (b) Zoom of (a) during the high-temperature period at the beginning of March 2023 with air temperatures included.*

533 We use the improved PDD to estimate surface melt based on the observed (for 280 m and 900 m  
 534 elevations) or reconstructed (for 600 m elevation) ice surface temperatures. The results show that  
 535 of the three sites, surface melt only occurs at the lowest elevation site. The melt rate at the lowest-  
 536 elevation AWS is 5.6 mm/day and 6.4 mm/day on the 2nd and 3rd of March, respectively (Fig. S2).  
 537 No surface melt was recorded at the AWS at 600 m or 900 m elevation. While we cannot rule out  
 538 that some of the surface meltwater penetrated to the bed of the glacier and mixed with the basal  
 539 meltwater, we consider this to be unlikely for the following reasons. Firstly, visual inspection of

540 the glacier surface during our field campaign revealed dry crevasses (Fig. S3a), icicles (Fig. S3b),  
541 refrozen puddles of water (Fig. S3c) and snow pockets on the surface (Fig. S3d); all suggesting that  
542 water forming on the surface refreezes again. Secondly, previous studies suggest that meltwater can  
543 be stored and refrozen in the weathered glacier surface and the surface snow [38]. Finally, scrutiny  
544 of remote sensing images showed no evidence of surface water transport or drainage systems.

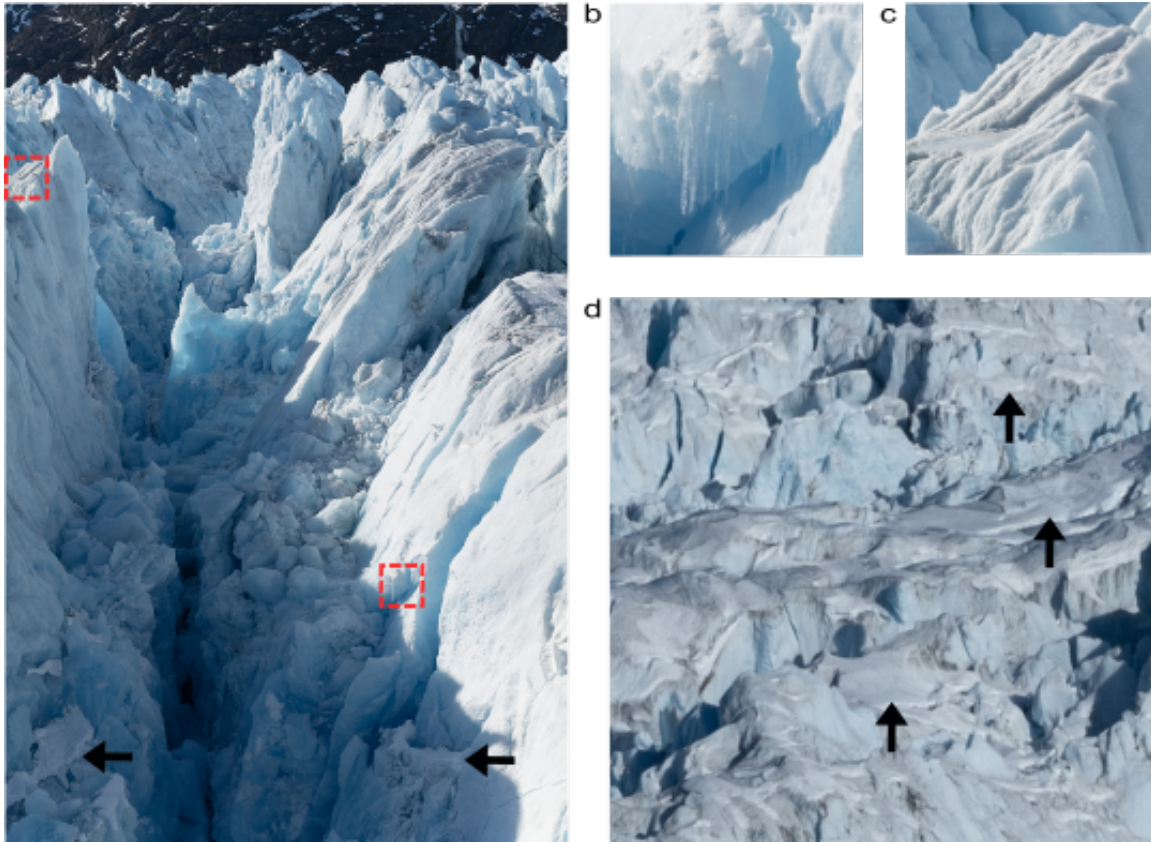


Figure S3: Pictures of Eqalorutsit Kangilliit Sermiat taken from a helicopter by S. Rysgaard on the 27th of March 2023. (a) Crevasse photographed from the side. The red squares show the location of (b) and (c). The black arrows point to some of the snow pockets. (b) Magnification of icicles in (a). (c) Magnification of a refrozen puddle of water in (a). (d) Glacier surface photographed from above. The black arrows point to some of the snow pockets.

### 545 Ice-marginal lake change

546 A time series of surface areas was derived for the five ice-marginal lakes identified between January  
547 and April 2023 (Fig. S4a). The five lakes were delineated manually across 21 timesteps using  
548 GEEDit [62]. Our dataset consists of 17 scenes from Sentinel-2 (10 m spatial resolution) and six  
549 scenes from Landsat 9 (30 m spatial resolution), and all scenes had less than 50% cloud cover (Fig.  
550 S4b). Occlusion of lake outlines occurred in some scenes due to localized cloud cover. The error  
551 estimate in lake surface area was quantified by repeated manual delineation of the Nordbosø lake

552 from the first Sentinel-2 and Landsat 9 image in the time series, returning an error estimate of  $\pm 4.5\%$   
 553 and  $\pm 6.3\%$ , respectively. The time series presented in Fig. S4b suggests that the five ice-marginal  
 554 lakes in this region experienced limited variability in the areas between January and April 2023.  
 555 There is no evidence of any glacier lake outburst flood or full drainage events from the five lakes.  
 556 The highest value in surface lake area is evident at the beginning of the time-series record, which  
 557 likely reflects the high snow cover at the start of the year. Generally, the variability in lake areas is  
 558 low in the latter half of the time series, coinciding with higher data coverage, particularly from the  
 559 Sentinel-2 record. The smaller lakes exhibit small changes across the time series; for example, Lake  
 560 1644 had a mean surface area of  $0.23 \text{ km}^2$ , varying between  $0.19 \text{ km}^2$  (Sentinel-2 delineation) and  
 561  $0.29 \text{ km}^2$  (Landsat 9 delineation), and a standard deviation of  $0.03 \text{ km}^2$ . Nordbosø Lake (lake ID  
 562 1897) exhibits the largest changes, primarily reflecting its size relative to the other lakes presented  
 563 here. Lake area was stable and consistent during our field campaign and the month preceding, with  
 564 an average standard deviation of  $0.062 \text{ km}^2$  in March (compared to an average standard deviation of  
 565  $0.166 \text{ km}^2$  over the entire time series). Thus, we conclude that there is no evidence of ice-marginal  
 566 lake drainage in our study area.

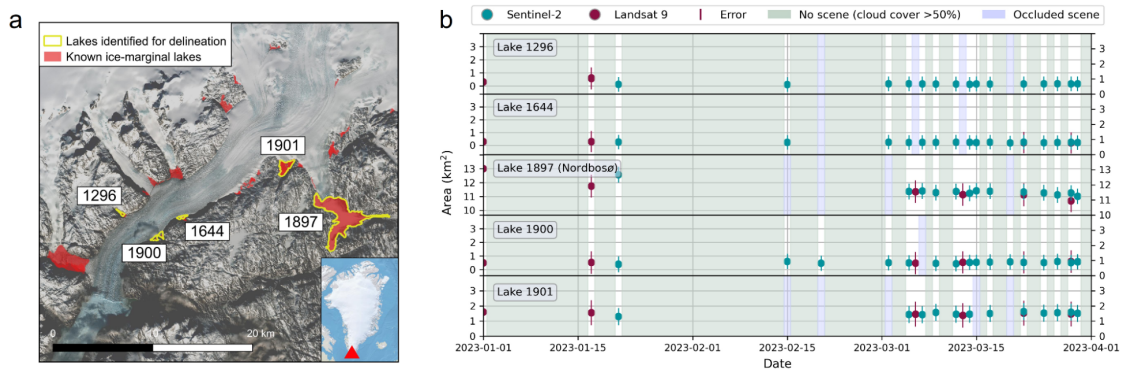


Figure S4: (a) The five ice-marginal lakes identified between January and April 2023 within the Eqalorutsit Kangilliit Sermiat catchment area and (b) the corresponding time-series of lake area change from Sentinel-2 and Landsat 9 imagery. Known ice-marginal lakes and lake identification numbers follow those defined by the 2017 inventory of Greenland ice-marginal lakes [44]. The background image in (a) is a visible composite from Sentinel-2 imagery captured on 6th March 2023.

## 567 Freshwater pool extent and volume

568 We estimate the size of the under-ice freshwater pool by assuming that the pool extends across the  
 569 entire glacier front but does not extend to St. 3. We base this assumption on the fact that we did  
 570 not observe any sign of subglacial discharge at St. 3. Thus, the lake must be situated between St.  
 571 3 and the glacier front, and our suggested outline indicates a likely maximum extent. The size of  
 572 the pool is outlined in Fig. S5 and estimated at  $14 \text{ km}^2$  area. Assuming that the under-ice lake  
 573 has uniform salinity conditions similar to those measured at St. 1 and St. 2, we can calculate the  
 574 amount of freshwater by integrating the difference between the average salinity profile of St. 1 and

575 St. 2 and the average salinity profiles from St. 3 and St. 4 down to 32 m depth where profiles  
 576 connect (Fig. 4). The under-ice lake freshwater reservoir amounts to  $2.38 \times 10^5 \text{ m}^3$ , an order of  
 577 magnitude smaller than the theoretically estimated monthly subglacial discharge due to basal melt.

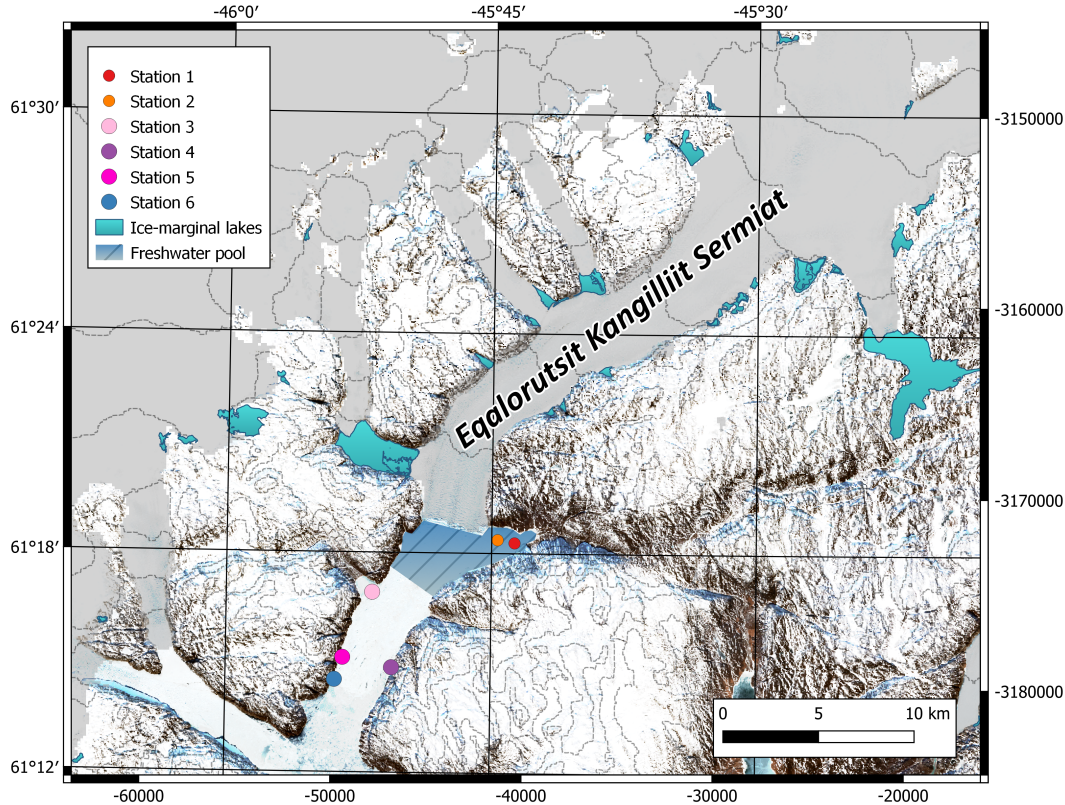


Figure S5: Map of Eqalorutsit Kangilliit Sermiat and surrounding areas. The suggested extent of the under-ice freshwater pool is indicated in dashed blue.

578 In addition to this estimate, we also investigated whether a numerical model developed for  
 579 summer plume studies [47] could be used to assess the volume of the freshwater pool. In brief, we  
 580 conclude that the model is not suited for our purposes partly due to the fact that it does not account  
 581 for freshening caused by icebergs and ice mélange, and partly due to the fact that our measurements  
 582 do not cover the entire depth of the glacier front. This is further described in the Supplementary  
 583 Materials.

## 584 Data availability

585 The measurements acquired in March 2023, the GINR measurement KR23034, the data acquired  
 586 in Nuup Kangerlua (GF10099), the estimates of ice-marginal lake extent (Fig S4) and high-resolution  
 587 versions of the photos presented in Fig. S3 are available at the GEUS Dataverse DOI: 10.22008/FK2/UHV7FF.  
 588 The data shown in Fig. S1 can be found at DOI: 10.22008/FK2/BOVBVR/6SU1Y6 while the AWS

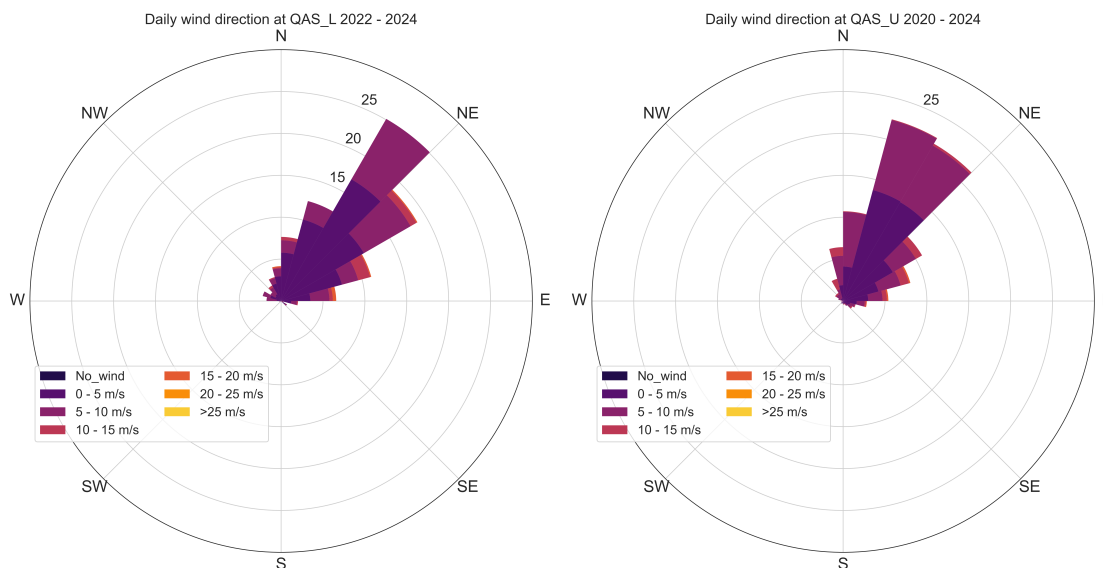


Figure S6: Measured daily wind directions from  $QAS_L$  and  $QAS_U$  from 2022 to September 2024. As shown, the prevailing wind direction is from the northeast.

589 data in Figs. S2 and S6 are available at <https://doi.org/10.22008/FK2/IW73UU>.

590

## 591 References

592 [59] Shreve, R. L. Movement of Water in Glaciers. *Journal of Glaciology* **11**, 205–214 (1972).

593 [60] How, P., Abermann, J., Ahlstrøm, A., A.P., S.B., B., J.E., Citterio, M., Colgan, W., Fausto,  
594 R., Karlsson, N., Jakobsen, J., Langley, K., Larsen, S., Lund, M., Mankoff, K., Pedersen, A.,  
595 Rutishauser, A., Shields, C., Solgaard, A., van As, D., Vandecrux, B. & Wright, P. PROMICE  
596 and GC-Net automated weather station data in Greenland (2022).

597 [61] Yang, X., Nielsen, K. P., Amstrup, B., Peralta, C., Høyer, J., Englyst, P. N., Schy-  
598 berg, H., Homleid, M., Køltzow, M. O., Randriamampianina, R., Dahlgren, P.,  
599 Støylen, E., Valkonen, T., Palmason, B., Thorsteinsson, S., Bojarova, J., Körnich,  
600 H., Lindskog, M., Box, J. & Mankoff, K. C3S Arctic regional reanalysis – Full sys-  
601 tem documentation. Tech. Rep., Copernicus Climate Change Service (2021). URL  
602 <https://datastore.copernicus-climate.eu/documents/reanalysis-carra/CARRAFullSystemDocumentationF>  
603 Last accessed 23 September 2024.

604 [62] Lea, J. M. The Google Earth Engine Digitisation Tool (GEEDiT) and the Margin change Quan-  
605 tification Tool (MaQiT) – simple tools for the rapid mapping and quantification of changing  
606 Earth surface margins. *Earth Surface Dynamics* **6**, 551–561 (2018).